Lithium Nitride for Reversible Hydrogen Storage

[*]Takayuki Ichikawa[1,2], Shigehito Isobe[2], Nobuko Hanada[2] and Hironobu Fujii[1,2]

1. *Natural Science Center for Basic Research and Development, Hiroshima University,*

Higashi-Hiroshima 739 - 8526, Japan,

2. *Graduate School of Advanced Sciences of Matter, Hiroshima University,*

Higashi-Hiroshima 739-8521, Japan

Abstract

In this paper, we examined the basic properties in the 1:1 mixture of lithium amide $LiNH_2$ and lithium hydride LiH as a candidate of reversible hydrogen storage materials. The thermal desorption mass spectra of the ball milled mixture without any catalysts indicated that hydrogen H_2 is released in temperature range from 180 to 400 ℃ with emitting a considerable amount of ammonia NH_3. On the other hand, the ball milled mixture containing a small amount of $TiCl_3$ as a catalyst showed the most superior hydrogen storage properties among the 1:1 mixtures with a small amount of catalysts, Ni, Fe, Co metals and $TiCl_3$ (1 mol.%). That is, the product desorbs a large amount of hydrogen (~5.5 wt.%) in the temperature from 150 to 250 ℃ under the condition of a heating rate of 5 ℃/min, but it does not desorb ammonia at all within our experimental accuracy. In addition, we confirmed that the product shows an excellent cycle retention with an effective hydrogen capacity of more than 5 wt.% and a high reaction rate until at least 3 cycles.

---

[*] Corresponding author.
E-mail address: tichi@hiroshima-u.ac.jp (T. Ichikawa)

Introduction

Recently, hydrogen energy systems have been proposed as a means to reduce greenhouse gas and other harmful emissions from stationary and mobile sources, aiming at a higher energy independence from fossil fuels. For realizing hydrogen energy systems in the near future, we have to establish suitable energy storage and transportation technologies. One of the key technologies on that way is in the development of high performance hydrogen storage (H-storage) materials [1,2].

So far, much attention has been paid to the hydrogen storage materials with light weight e.g. light metal hydrides [3-6], chemical hydrides[7-14] and carbon related materials[15-18]. Until now, we have studied Mg-based metal hydrides[19-21] and carbon related material systems [22-24] with high hydrogen absorption capacity to improve the hydrogen desorption properties.

Quite recently, lithium nitrides absorbing/desorbing a large amount of hydrogen have been reported by P. Chen et al.[25] as a candidate of reversible hydrogen storage materials. The reaction is as follows:

$$Li_3N + 2H_2 \Leftrightarrow LiNH_2 + 2LiH \qquad (1),$$

$$\Delta H = -96.3 \text{ kJ/mol } H_2.$$
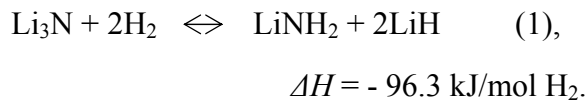
Theoretically, reversible hydrogen of 10.4 wt.% $(2H_2/(Li_3N+2H_2))$ can be stored in this reaction. In details, Chen et al. claimed that the above hydrogen storage involved the following clear two-step reaction path:

$$Li_3N + H_2 \Leftrightarrow Li_2NH + LiH \qquad (2),$$

$$\Delta H = -165 \text{ kJ/mol } H_2,$$

and

$$Li_2NH + H_2 \Leftrightarrow LiNH_2 + LiH \qquad (3),$$

$$\Delta H = -44.5 \text{ kJ/mol } H_2.$$
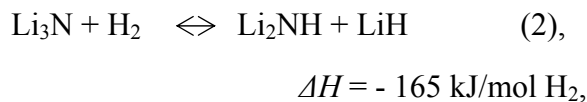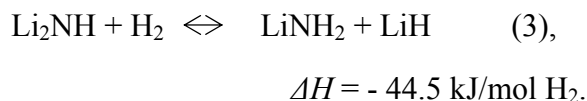
This indicates that reaction (3) can more easily absorb/desorb 6.5 wt.% of hydrogen because of the smaller negative enthalpy change ΔH upon hydrogen uptake. But, if we

choose Li₃N as a starting material for hydrogen storage, the hydrogenated materials are finally decomposed into $LiNH_2$ and $2LiH$, where the excess LiH could not be responsible for hydrogen storage in reaction (1) as is clear from reaction (3). In this case, only ~5.2 wt.% of hydrogen can be reversibly stored in the material starting from Li₃N.

To realize reaction (3) for hydrogen storage, we chose $LiNH_2$ and LiH as starting materials. In this paper, we examined the hydrogenation/dehydrogenation properties of a powder mixture of $LiNH_2$ and LiH, and also examined the catalytic effect on hydrogen storage properties for improving the kinetics of the reaction.

2. Experimental

The starting materials, LiH and $LiNH_2$ with 95 % purity were purchased from Sigma-Aldrich and from Strem Chemicals, respectively. The dry catalyst metals Fe, Co, Ni with diameter of several tens of nanometers were from Shinku-Yakin, and $TiCl_3$ was from Sigma-Aldrich. All the samples were handled in a glove−box filled with purified argon to minimize oxidation and water adsorption.

For the purpose of comparing the conditions of nanometer-scale contact between $LiNH_2$ and LiH, the mixed powders were prepared in two different ways. In one case the mixing was done with an agate mortar and pestle by hand and in the other case we used mechanical ball milling (Fritsch P7). In the former case, 300 mg of $LiNH_2$ and LiH powders with 1:1 and 1:2 molar ratios were mixed for ten minutes. In the latter case, 300 mg of the powders were mixed with the same ratio for 2 hrs. In the milling process, the powders and 20 pieces of steel balls with a diameter of 7 mm were brought into a Cr steel pot, and milled with 400 rpm for 2 hrs under a hydrogen gas pressure of 1 MPa at room temperature.

To clarify the catalytic effect on hydrogen storage properties, a small amount of Ni, Fe, Co metals and $TiCl_3$ (1 mol.%) were added to the powders of $LiNH_2$ and LiH before ball milling, and then these were ground by mechanical ball milling method for 2 hrs.

After homogenizing the mixed powders by the above methods, the samples were

examined by thermal desorption mass spectroscopy (TDMS) (Anelva M-QA200TS) combined with thermogravimetry (TG) upon heating up to 450 ℃ with a heating rate of 5 ℃/min. This equipment was especially designed and built up for using it inside the glove box filled with purified argon, which permitted simultaneous measurements by TG and TDMS without exposing the samples to air at all. Before and after performing the TG-TDMS measurement, we examined the structures of the products by the X-ray diffraction (XRD) measurements (Rigaku RINT2000, Cu Kα).

3. Results and discussion

Figure 1 shows thermal desorption mass spectra (TDMS) of hydrogen (H_2) and ammonia (NH_3) gases for three kinds of $LiNH_2$ and LiH mixed powders. Samples 1 and 2 were both mixed using an agate mortar and pestle by hand for ten minutes. The mixing ratio of $LiNH_2$ and LiH is 1:1 in the sample 1, while it is 1:2 in the sample 2. Sample 3 was prepared by mechanically milling the 1:1 mixture of $LiNH_2$ and LiH. We can easily notice that ammonia gas in addition to hydrogen gas is desorbed from all the mixed powders as well. The amount of desorbed NH_3 gas decreases with increasing the ratio of LiH to $LiNH_2$ for the hand mixed powders. We also notice that the amount of NH_3 from the ball milled powder is much less than when using the agate mortar for the mixing.

Usually, the ammonia gas is irreversibly released by the following decomposition reaction:

$$2LiNH_2 \rightarrow Li_2NH + NH_3 \qquad (4),$$
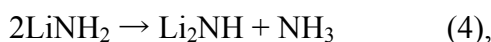
$$\Delta H = 84.1 \text{ kJ/mol } NH_3.$$

The TDMS of ammonia from pure $LiNH_2$ powder was examined in this work, as shown in Figure 2. One can see that the ammonia gas is drastically desorbed starting at ~300 ℃.

This reaction indicates that, if $LiNH_2$ closely touches LiH in a nanometer scale in the mixed powder, the desorbing reaction of hydrogen (3) occurs before $LiNH_2$

decomposes into Li_2NH and NH_3 according to the reaction (4). It should be noted that the peak temperature of the hydrogen desorption from sample 3 is lowest among the above three samples, ensuring such a good contact between $LiNH_2$ and LiH by ball milling. However, since the reaction rate is still low, a small amount of unreacted $LiNH_2$ remains near 300 ℃, where $LiNH_2$ starts to decompose into Li_2NH and NH_3. It seems likely that the desorption of a small portion of hydrogen at higher temperature than 300 ℃ occurs simultaneously with the emission of ammonia gas.

Figure 3 shows X-ray diffraction profiles of the sample 3(a) ground the 1:1 mixture of $LiNH_2$ and LiH by ball milling without any heat treatments, and the sample 3(b) after heating sample 3(a) up to 450 ℃ and desorption of the hydrogen. We notice that the XRD patterns of Li_2NH and $LiNH_2$ phases are quite similar to each other. Therefore, it is quite difficult to check the dehydrogenating reaction only from the XRD patterns. Then, we checked the occurrence of reaction (3) from the existence of the XRD peaks of the LiH phase in the above two samples, which only exists in the pattern of sample 3(a). For both the samples, we can easily notice a considerable amount of $LiOH$ contamination in the XRD patterns, which may originate from moisture in the air during the XRD measurement.

Next, we examined the catalytic effect on hydrogen storage properties for the ball milled powder with a 1:1 molar ratio of $LiNH_2$ and LiH. As effective catalysts for improving the reaction rate, a small amount of Ni, Fe, Co metals and $TiCl_3$ (1 mol.%) were chosen and added to the 1:1 mixture of $LiNH_2$ and LiH before the ball milling, and then ball milling was done for 2 hrs. Figure 4 shows the TDMS for hydrogen (H_2) and ammonia (NH_3) gases from the mixed powders containing a small amount of Ni, Fe, Co metals and $TiCl_3$ (1 mol.%) as catalysts. The mixture containing a small amount of $TiCl_3$ as catalyst shows the most superior hydrogen storage properties among the mixtures, where the product shows the sharpest hydrogen desorption curve and desorption of a large amount of hydrogen (~5.5 wt.%) in the temperature from 150 to 250 ℃ using a heating rate of 5 ℃/min. This indicates that the reaction rate is

dramatically improved by adding 1 mol.% of $TiCl_3$ as a catalyst, leading to lower activation energy for reaction (3) than in the mixture without catalyst. Here, it is noteworthy that no ammonia gas emission is detected at all in the TDMS measurement up to 450 ℃ for the 1:1 mixture with 1 mol.% of $TiCl_3$ as a catalyst within our experimental accuracy. This result indicates that all of the $LiNH_2$ has already been consumed as a result of reacting with LiH and transforming into Li_2NH at the final point of hydrogen desorption, leading to no ammonia gas emission at all . Also, it is to be noted that the hydrogen desorption capacity (~5.5 wt.%) is lower than the theoretical hydrogen content of 6.5 wt.%. This may be due to the existence of stable impurity phases of Li_2O and LiOH in the raw compounds $LiNH_2$ and LiH we purchased.

Furthermore, we have investigated the kinetics of the dehydriding reaction for the 1:1 ball milled mixture containing 1 mol.% of $TiCl_3$. Figure 5 shows the logarithmic plot of the normalized residual hydrogen amount $X_{H2}(t)/X_{H2}(0)$ and the linear plot of the measuring temperature as a function of time for the powders ball milled with and without 1 mol.% $TiCl_3$ catalyst. One can see that the reaction rate of the product with the catalyst is much faster than that without the catalyst and both logarithmic plots are linear against time after the measuring temperature reached a fixed point and became constant, indicating that the reaction is of first order. If so, we can easily obtain the activation energy, E_a, for the hydrogen desorption reaction according to Kissinger's method [26]. In Figure 6(a), the TDMS measured by changing the heating rates from 1 K/min to 20 K/min are plotted as a function of temperature, and the Kissinger plot is given in Figure 6(b). The value of E_a is deduced to be 110 kJ/mol from the Kissinger plot. This value is still high compared to that deduced for catalyzed sodium alanates [11]. This indicates that catalytic effects have to be optimized in the near future. On the other hand, the E_a for the non-catalyzed mixture could not be estimated because of the existence of complex desorption reactions of H_2 and NH_3 gases at higher heating rate.

Finally, we examined the cycle retention properties for the sample with the 1mol.% $TiCl_3$ catalyst. The durability was tested by the following cyclic processes: the

dehydrogenation was performed by holding the sample at 220 ℃ for 12 hrs under high-vacuum, and then the hydrogenation was performed under pure hydrogen gas up to 3 MPa at 180 ℃ for 12hrs. After these hydrogen absorbing/desorbing cycles, we examined the hydrogen desorption properties by TG-TDMS measurements. The results obtained are shown in Figure 7. The amount of desorbed hydrogen decreases slightly after the 2nd cycle, indicating that a small amount of stable materials, that is Li_2O, TiN or LiCl, may have been generated during the first heating process. However, since the effective hydrogen capacity is still higher than 5 wt.% after the initial dehydrogenation process, and the reaction rate has almost not changed until at least the 3rd cycle, we can say that the cycle retention is not so bad.

4. Conclusion

We examined the hydrogenating/dehydrogenating properties of a 1:1 mixture of $LiNH_2$ and LiH catalyzed by 1 mol.% of $TiCl_3$ prepared by ball milling. The product desorbs a large amount of hydrogen (~5.5 wt.%) in the temperature range from 150 to 250 ℃ upon heating (5 ℃/min) without emission of ammonia. Almost 80 % of total hydrogen content (~5.5 wt.%) is desorbed within 30 min. at ~200 ℃. We also confirmed that this system preserves its effective hydrogen capacity of more than 5 wt.% and its high reaction rate until at least 3 cycles. The above results indicate that a mixture of lithium amide $LiNH_2$ and lithium hydride LiH is one of the promising candidates for reversible hydrogen storage materials.

Japan.

References

1. E. Akiba, Curr. Opin. Solid State Mat. Sci. **4** (1999) 267.

2. L. Schlapbach, A. Züttel, Nature, **414** (2001) 353.

3. A. Zaluska, L. Zaluski, J. Ström-Olsen, J. Alloys Comp. **288** (1999) 217.

4. M. Okada, K. Kuriiwa, T. Tanuma, H. Takamura, A. Kamegawa, J. Alloy Comp. **330-332** (2002) 511.

5. L. Kanoya, M. Hosoe and T. Suzuki, *Honda R & D Technical Review,* **14** (2002) 91.

6. H. Fujii, K. Higuchi, K. Yamamoto, H. Kajioka, S. Orimo, K. Toiyama, Mater. Trans. **43** (2002) 2721.

7. B. Bogdanovic and M. Schwickrdi, J. Alloys Comp. **253** (1997) 1.

8. B. Bogdanovic, R.A. Brand , A. Marjanovic, M. Schwickardi, J. Tölle, J. Alloys Comp. **302** (2000) 36

9. C.M. Jensen, K.J. Gross, Appl. Phys. **A, 72** (2001) 213

10. K.J. Gross, G.J. Thomas, C.M. Jensen, J. Alloys Comp. **330-332** (2002) 683

11. G. Sandrock, K. Gross, G. Thomas, J. Alloys Comp. **339** (2002) 299.

12. M. Fichtner, O. Fuhr, J. Alloys Comp. **345** (2002) 286

13. H. Morita, K. Kakizaki, S. Chung, A. Yamada, J. Alloys Comp. **353** (2003) 310

14. Z. P. Li, B.H. Liu, N. Morigasaki, S. Suda, J. Alloys Comp. **354** (2003) 243

15. A.C. Dillon, K. M. Jones, T. A. Bekkedahl, C. H. Kiang, D. S. Bethune, M. J. Heben, Nature (London) **386** (1997) 377.

16. A.C. Dillon, M.J. Heben, Appl. Phys. A, **72** (2001) 133

17. H.M. Cheng, Q.H. Yang, C. Liu, Carbon, **39** (2001) 1447

18. A. Chambers, C. Park, R.T.K.Baker & N.M.Rodrigues, Phys. Chem. **B102** (1998) 4253.

19. S. Orimo, H. Fujii, Intermetallics, **6** (1998) 185.

20. S. Orimo, H. Fujii, Appl. Phys. A, **72** (2001) 167.

21. N. Hanada, S. Orimo, H. Fujii, to be published in J. Alloys Comp.(2003)

22. S. Orimo, G. Majer, T. Fukunaga, A. Züttel, L, Schlapbach, H. Fujii, Appl. Phys. Lett. **75** (1999) 3093.

23. S. Orimo, T. Matsushima, H. Fujii, T. Fukunaga, G. Majer, J. Appl. Phys. **90** (2001) 1545.

24. D.M. Chen, T. Ichikawa, H. Fujii, N. Ogita, M. Udagawa, Y. Kitano, E. Tanabe, J. Alloys Comp. **354** (2003) L5.

25. P. Chen, Z. Xiong, J. Luo, J. Lin, K.L. Tan, Nature **420** (2002) 302.

26. H.E. Kissinger, Anal. Chem. **29** (1957) 1702.
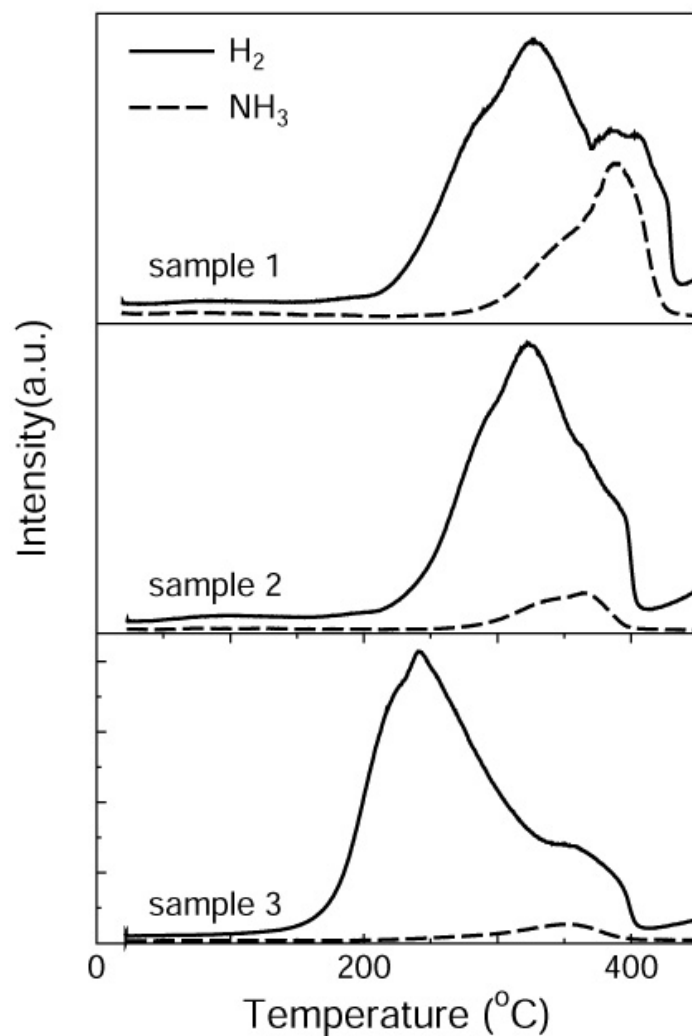
Figure 1. Thermal desorption spectra of hydrogen (real line) and ammonia (dash line) from mixed $LiNH_2$ and LiH powders under constant heating rate (5 ℃/min): Samples 1 and 2 were mixed using agate mortar and pestle and sample 3 were mixed by ball milling. The molar ratio of LiH to $LiNH_2$ is 1:1 for samples 1 and 3, and 1:2 for sample 2.
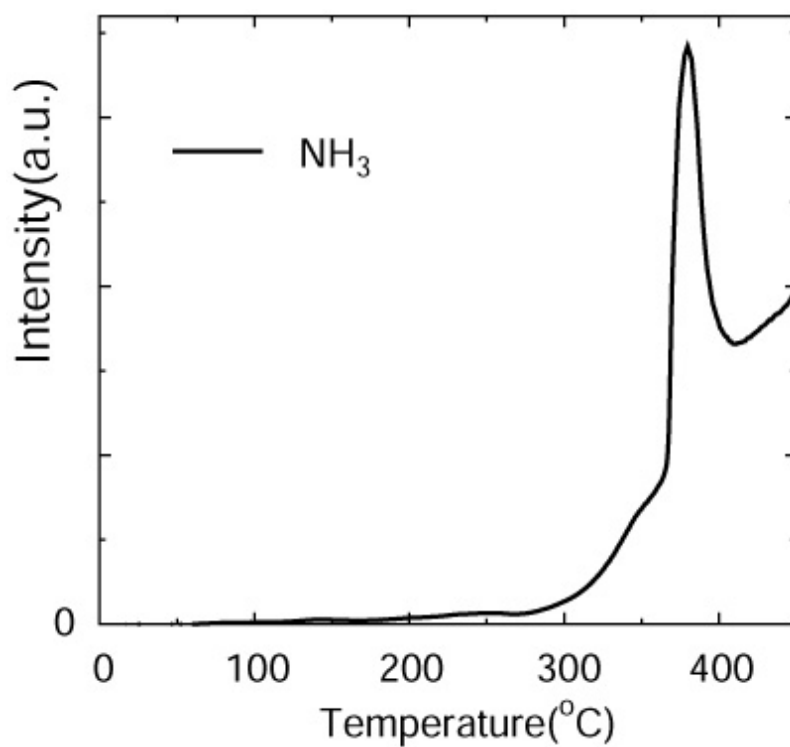
Figure 2. Thermal desorption spectrum of ammonia from pure LiNH$_2$ powder under constant heating rate (5 $^\circ$C/min)
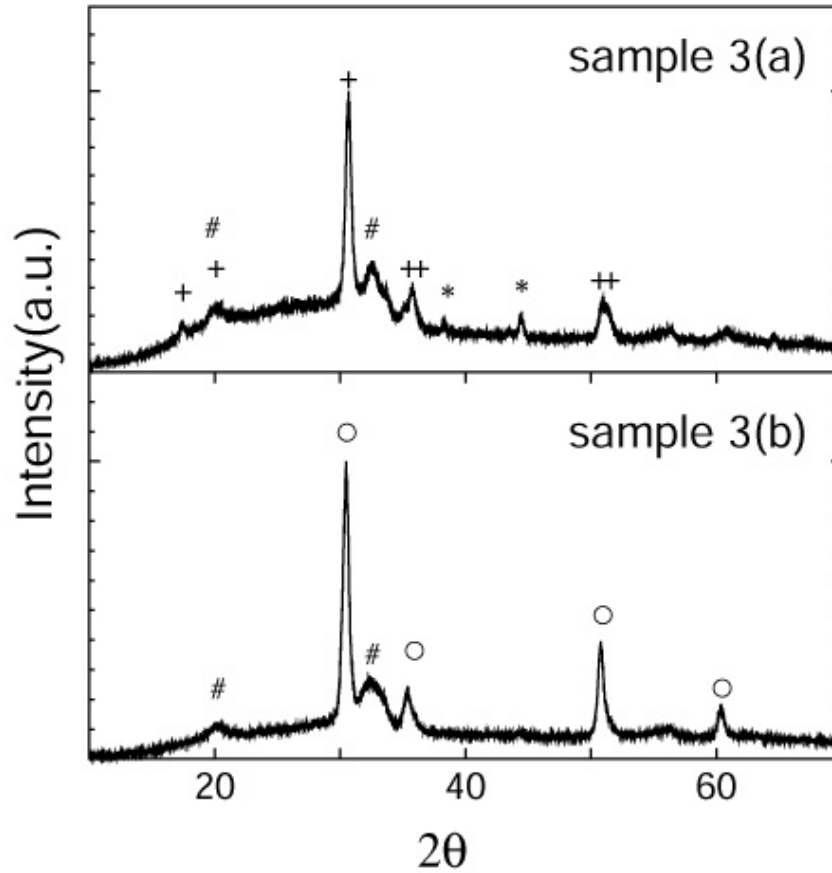
Figure 3. X-ray powder diffraction patterns of sample 3(a) which is a 1:1 ball milled mixture of $LiNH_2$ and LiH before heat treatment and sample 3(b) which was obtained after heating up to 450 ℃ ; +:$LiNH_2$, *:LiH, ○:Li_2NH, #:$LiOH$. The back ground broad maximum in the XRD profiles is due to grease used for fixing the samples on the glass substrate.
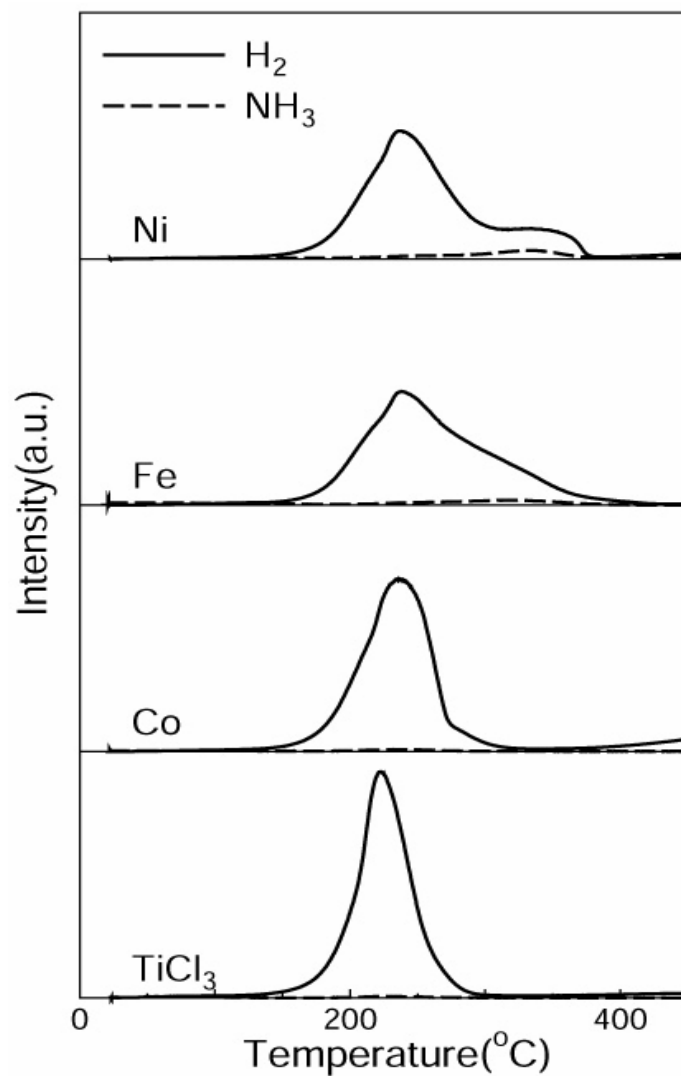
Figure 4. Thermal desorption spectra of hydrogen and ammonia from the 1:1 ball milled mixtures of $LiNH_2$ and LiH, in which a small amount (1 mol.%) of Ni, Fe and Co nano-size metals, and $TiCl_3$ are added as catalysts before milling.
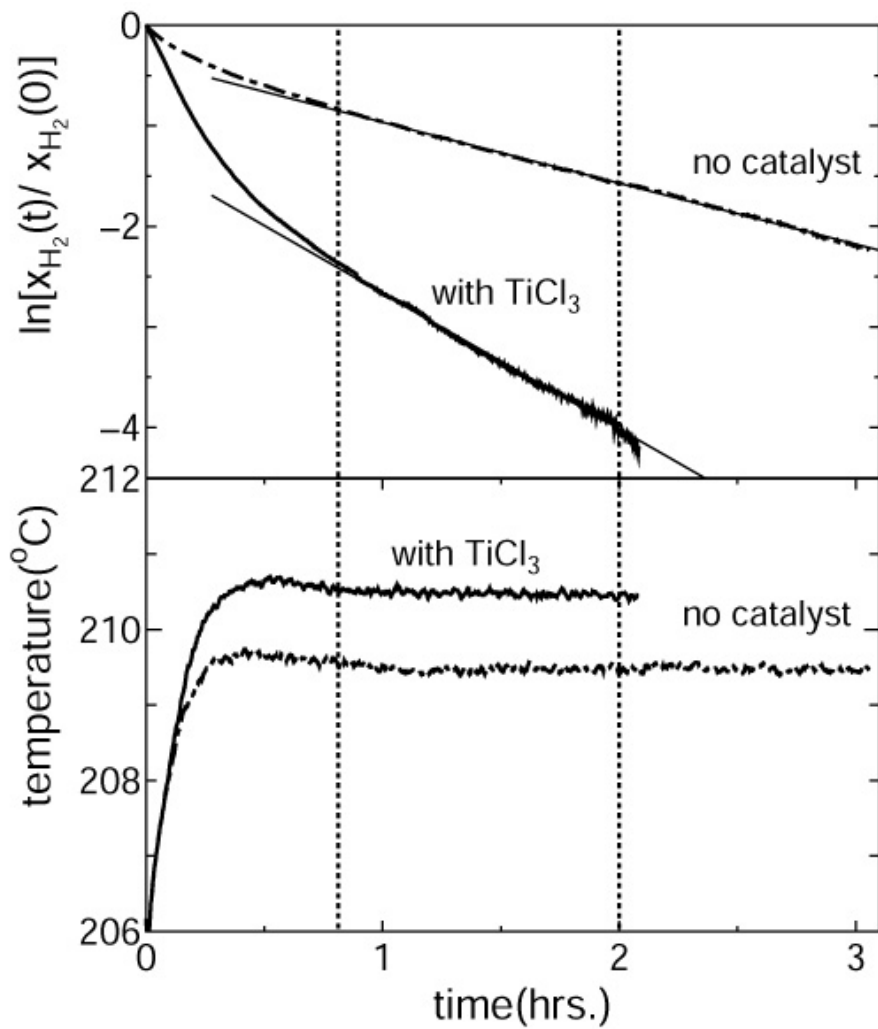
Figure 5. Logarithmic plots of normalized residual hydrogen amount, $X_{H2}(t)/X_{H2}(t)$, and linear plots of measuring temperature as a function of time for the 1:1 ball milled powders with and without 1 wt.% $TiCl_3$ catalyst.

(a)

(b)
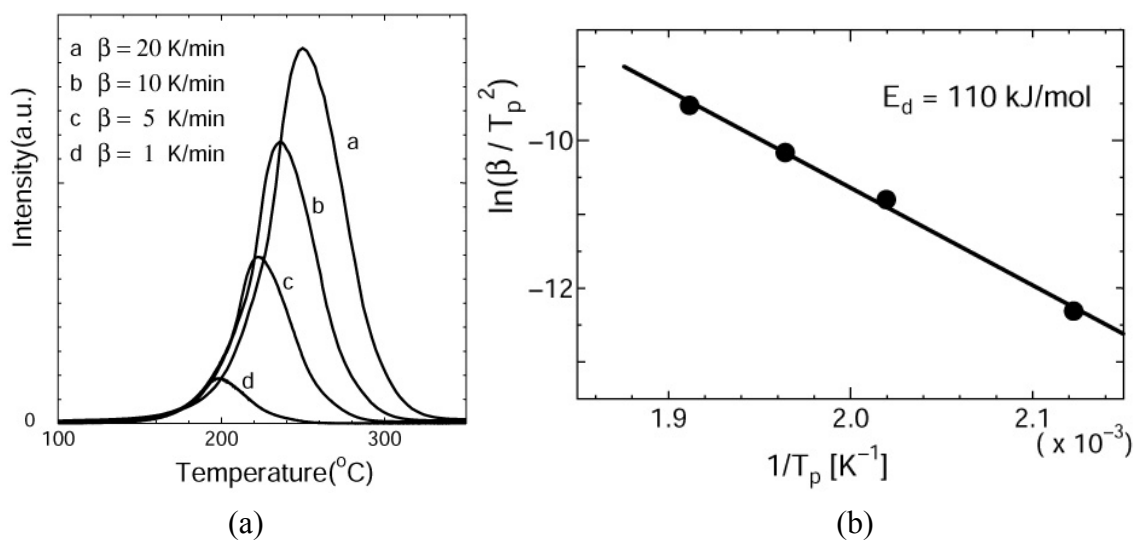
Figure 6. (a) Thermal desorption spectra of hydrogen under various heating rates (β =1, 5, 10, 20 ℃/min) from the 1:1 ball milled mixture of LiNH₂ and LiH catalyzed with a small amount (1 mol.%) of TiCl₃, and (b)Kissinger plot of the hydrogen desorption. Notations: T_p indicates the peak temperatures (198, 222, 236, 250 ℃) of thermal desorption spectra (a). The solid line represents a least square fitting of the data. From this slope, we could obtain the activation energy E_d = 110 kJ/mol.
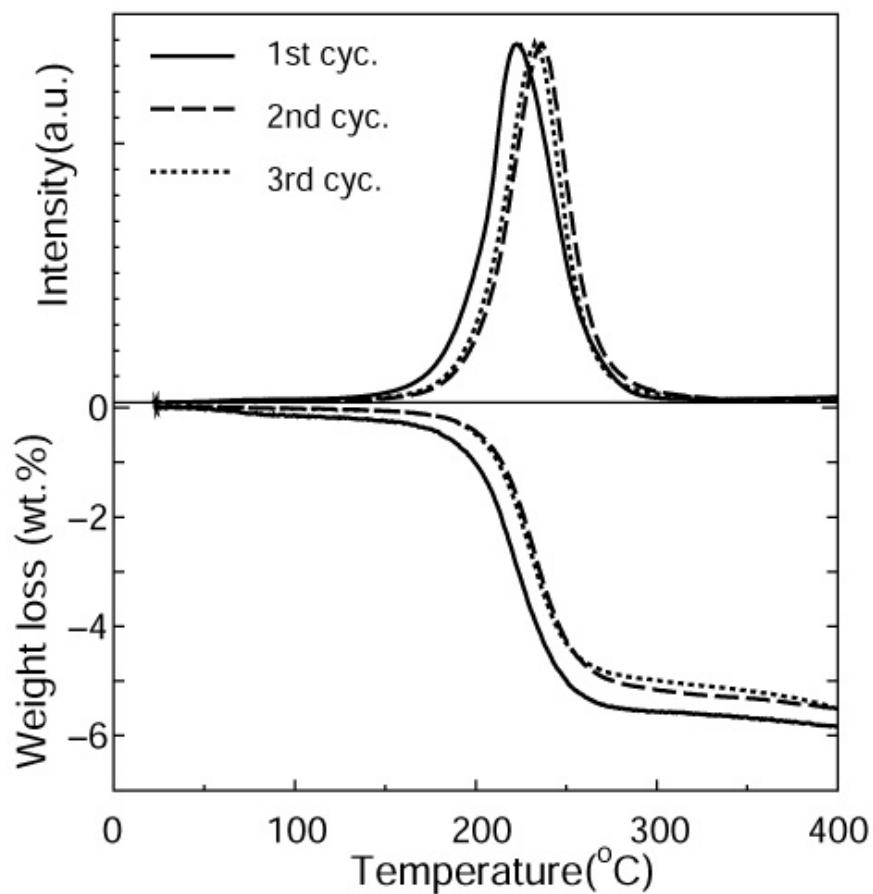
Figure 7. Thermal desorption spectra of hydrogen from the 1:1 mixture of LiNH$_2$ and LiH catalyzed with a small amount (1 mol.%) of TiCl$_3$ which were mixed by ball milling.